Osteoporosis International (2019) 30:2257–2269
https://doi.org/10.1007/s00198-019-05086-4

ORIGINAL ARTICLE

Evaluation of bone texture imaging parameters on panoramic radiographs of patients with Sheehan's syndrome: a STROBE-compliant case-control study

D. de Sá Cavalcante[1] · M.G. da Silva Castro[2] · A.R.P. Quidute[3] · M.R.A. Martins[3] · A.M.P.L. Cid[1] · P.G. de Barros Silva[1] · J. Cadwell Williams Jr[4] · F.S. Neves[5] · T.R. Ribeiro[1] · F.W.G. Costa[1]

Received: 28 November 2018 / Accepted: 9 July 2019 / Published online: 2 August 2019

Abstract

Summary Sheehan's syndrome (SHS) is a rare condition related to the risk of osteoporosis and evaluation of bone texture imaging features on panoramic radiographs would be suitable for this condition, which was the aim of the present study. Fractal dimension, lacunarity, and trabecular morphologic aspects were significantly altered in these patients.

Introduction SHS is an important public health problem particularly in developing countries. It is characterized as postpartum hypopituitarism secondary to obstetric complications-related ischemic pituitary necrosis that shows significant systemic metabolic repercussions. Thus, this study aimed to evaluate bone texture parameters in digital panoramic radiographs of patients with SHS.

Methods A case-control study was conducted with 30 SHS patients from an Endocrinology and Diabetology Service of reference in Brazil, and 30 age- and sex-matched healthy controls. A custom computer program measured fractal dimension, lacunarity, and some morphologic features in the following mandibular regions of interest (50 × 50 pixels): below the mental foramen (F1), between the first and second molars (M1), and at the center of the mandibular ramus (R1).

Results The fractal analysis showed a statistically significant difference between the studied groups in all regions of interest. The fractal dimension in F1 ($p = 0.016$), M1 ($p = 0.043$), and R1 ($p = 0.028$) was significantly lower in SHS group, as well as lacunarity in R1 ($p = 0.008$). Additionally, several morphologic features were statistically significant in the SHS group ($p < 0.05$).

Conclusion Therefore, individuals with SHS showed altered imaging texture parameters on panoramic radiographs, which reflect a smaller spatial organization of the bone trabeculae and, possibly, a state of reduced mineral bone density.

Keywords Sheehan's syndrome · Texture imaging parameters · Mineral bone density · Panoramic radiograph

Introduction

The role of the pituitary-bone axis in skeletal pathophysiology has been widely recognized throughout the last decades [1]. Pituitary hormones play an important connection with skeleton-related bone metabolism because bone cells usually express hormone receptors for growth hormone, follicle-stimulating hormone, thyroid stimulating hormone, adrenocorticotrophic hormone, prolactin, oxytocin, and vasopressin, and their roles are evident especially in several diseases [2, 3]. Among the

Electronic supplementary material The online version of this article (https://doi.org/10.1007/s00198-019-05086-4) contains supplementary material, which is available to authorized users.

✉ F.W.G. Costa
fwildson@yahoo.com.br

[1] Department of Clinical Dentistry, Postgraduate Program in Dentistry, Federal University of Ceará, Alexandre Baraúna St 949, Rodolfo Teofilo, Fortaleza, Ceará 60430-160, Brazil

[2] Realistic Simulation Center, Univeristy Center UNICHRISTUS, R. João Adolfo Gurgel St 133, Cocó, Fortaleza, Ceará 60190-060, Brazil

[3] Division of Endocrinology and Diabetology, Walter Cantídio University Hospital, Alexandre Baraúna St 949, Rodolfo Teofilo, Fortaleza, Ceará 60430-160, Brazil

[4] Department of Anatomy and Cell Biology, Indiana School of Medicine, 635 Barnhill Dr, Indianapolis, IN 46202, USA

[5] Division of Oral Radiology, School of Dentistry, Federal University of Bahia, Araújo Pinho ave 62, Canela, Salvador, Bahia 40110-040, Brazil

disturbances that can affect the pituitary gland, Sheehan's syndrome (SHS) is a disease that affects the secretion of adenohypophyseal hormones. This condition is known as postpartum pituitary necrosis, and it is a rare condition that was first reported in 1937 by HL Sheehan, who described 12 cases of gland necrosis and pituitary failure following obstetric complications [4].

SHS is characterized by a hormonal insufficiency due to hypovolemia secondary to an excessive loss of blood during or even after delivery, which may be a result from glandular hyperplasia during pregnancy caused by the greater production of gestational hormones during this period [5] In this situation, the gland becomes more vulnerable to a total or partial necrosis due to ischemia caused by hypovolemic shock, since poor blood supply to the anterior region of the pituitary gland impairs its function because of possible ischemia during or after childbirth [5, 6]. Clinically, these findings are seen as hormonal deficiency, which occurs with an individual variability, ranging from impairment of a single tropic hormone to classic panhypopituitarism [7], and SHS patients may develop a spectrum of manifestations, such as agalactia (failure of postpartum lactation), amenorrhea (failure of postpartum menstruation), adynamia (muscle weakness), adrenocortical insufficiency, clinical findings related to secondary hypothyroidism, fine wrinkling around the mouth and eyes, diabetes insipidus, and empty sella [8].

Progressive loss of pituitary gland function in SHS decreases the secretion of bone metabolism-related hormones such as growth hormone (GH), follicle-stimulating hormone (FSH), luteinizing hormone (LH), thyroid stimulating hormones, adrenocorticotrophic hormone, cortisol, estradiol, and prolactin [9]. Serum levels of LH, FSH, and estradiol are considerably decreased in patients with SHS so that hypogonadism may be one of the possible mechanisms of osteoporosis in these patients. The reduction of GH levels has a significant effect on bone metabolism and plays a crucial role in the maintenance of bone mass in adults, regulating bone remodeling [5]. It is presumed that by reducing the secretion of hormones involved in the regulation of bone metabolism in patients with SHS, the maxillomandibular complex may present varying degrees of osteopenia or even osteoporosis.

In spite of epidemiological studies regarding clinical symptoms observed in SHS [10–12], recent investigations have focused on the bone microarchitecture and its osteoporotic pattern. Agarwal et al. [13] evaluated a large group of women with SHS and found low bone mass among these individuals after assessment by dual-energy X-ray absorptiometry (DXA). This is an available modality to assess bone mineral density. However, other medical imaging technologies have been proposed as including magnetic resonance imaging, transiliac crest bone biopsy-related micro-computed tomographic analysis, high-resolution peripheral quantitative computed tomography (HRpQCT), 2D X-ray images-related texture analysis, and trabecular bone score obtained from standard lumbar spine DXA images [14]. Morphologic characteristics are obtained through routine oral and maxillofacial radiology approach such as bone textural analysis in dental radiographs [15] and computed tomography [16]. Panoramic radiographs are commonly requested during routine dental examinations and have been used as an additional screening tool for low mineral bone density through fractal dimension.

Fractal analysis is a non-invasive, reliable, economical, and easy applicable method to obtain data of bone microarchitecture, and has been used in several studies in the field of dentomaxillofacial radiology [17–19]. Based on bone fractal properties (self-similarity and lack of well-defined scale), fractal analysis was considered as a beneficial method to evaluate the structural status of the trabecular bone [20], and numerical representation of fractal dimension was not affected by variations in X-ray exposure, small variations in beam alignment, and choice of the region of interest (ROI) [21].

Fractal dimension of the trabecular bone has been shown altered in osteoporotic postmenopausal women [22], which highlights its potential diagnostic value for detecting bone abnormalities in underlying disorders. In endocrine pathologies, fractal analysis and other textural imaging tools such as lacunarity and morphologic aspects were successful in evaluating osteoporosis [22, 23], osteogenesis imperfecta [20], hyperparathyroidism [24], chronic renal failure [19], sickle cell anemia [25], and diabetes mellitus [26]. Reports have indicated panoramic radiograph-related mean fractal dimension ranging from 1.02 [20] to 1.68 [25], and lacunarity ranging from 0.34 to 0.41 [18] in patients with bone disorders, while the cutoff values of these parameters like those of bone mineral density have not been obtained yet.

To date, there are no published reports evaluating these parameters in panoramic radiographs of SHS individuals. Thus, this investigation aimed to analyze panoramic radiograph texture features of SHS in comparison with non-syndromic pared individuals.

Materials and methods

Study design

A case-control study was conducted following Strengthening the Reporting of Observational studies in Epidemiology (STROBE) statements (https://www.strobe-statement.org/). The cases were represented by patients diagnosed with SHS under medical follow-up, and the controls were non-SHS individuals matched by sex and age.

Setting

Sample was obtained from the Endocrinology and Diabetology Service of the Walter Cantídio University Hospital (Fortaleza,

Ceará, Brazil), which concentrates a significant SHS casuistry in Brazil. It was recruited volunteers who were under follow-up for more than 10 years and volunteers matched by sex and age who agreed to participate in the study after reading, understood and signed a written informed consent form (research protocol # 983 022 approved by the Ethics Committee of the Federal University of Ceará).

Sample selection

The population included all patients presenting previous history of classic surgical-related hemorrhage and other obstetric and hormonal complications related to SHS diagnosis (n = 66). During the recruitment phase, it was included patients with a proven diagnosis of SHS under a routine ambulatory follow-up and those that consented to participate in this research. The individuals were excluded for any one of the following reasons: no attendance at routine medical appointments, no return of phone calls, death, or inability to perform panoramic radiography. After this phase, 30 volunteers were submitted to anamnesis, and they were required to perform digital panoramic radiography at the Dental Imaging Service of the Faculty of Pharmacy, Dentistry, and Nursing (Federal University of Ceará). In order to provide a case-control methodological design, for each case, a non-SHS sex- and age-matched volunteer that did not show any systemic alterations that could interfere in bone metabolism was recruited. Thus, 60 individuals participated in this study as shown in Fig. 1.

Quantitative variables

The quantitative variables assessed were fractal dimension, lacunarity, and morphological parameters related to the trabecular bone (trabecular area, periphery, total length of trabeculae, number of end points, and number of branching points).

Data sources/measurement

Obtaining and evaluating of digital panoramic radiographs

Standardized digital panoramic radiographs were obtained by using Kodak K9000 3D (Kodak Dental Systems, Carestream Health, Rochester, NY, USA) with a 14-bit grayscale (16384 greylevel), exposure time of 13.9 s, 65 kV, and 10 mA. Each patient was positioned using a chin rest and head stabilizer in the focal layer. A horizontal reference line was then superimposed on the patient's Frankfort horizontal plane as a technical standardization adopted during image acquisition. The Frankfort plane was positioned parallel to the ground and the median sagittal plane was perpendicular to the ground [27]. All obtained images were exported as TIFF (Tagged Image File Format), 300 dpi, and subsequently imported into the MATLAB R2016a program (The MathWorks, Inc., Natick, MA, USA). In order to calculate measurement errors, the study reliability was conducted through image evaluation during a 15-day interval. Also, to ensure the double-blind study design, a collaborator who did not evaluate the images

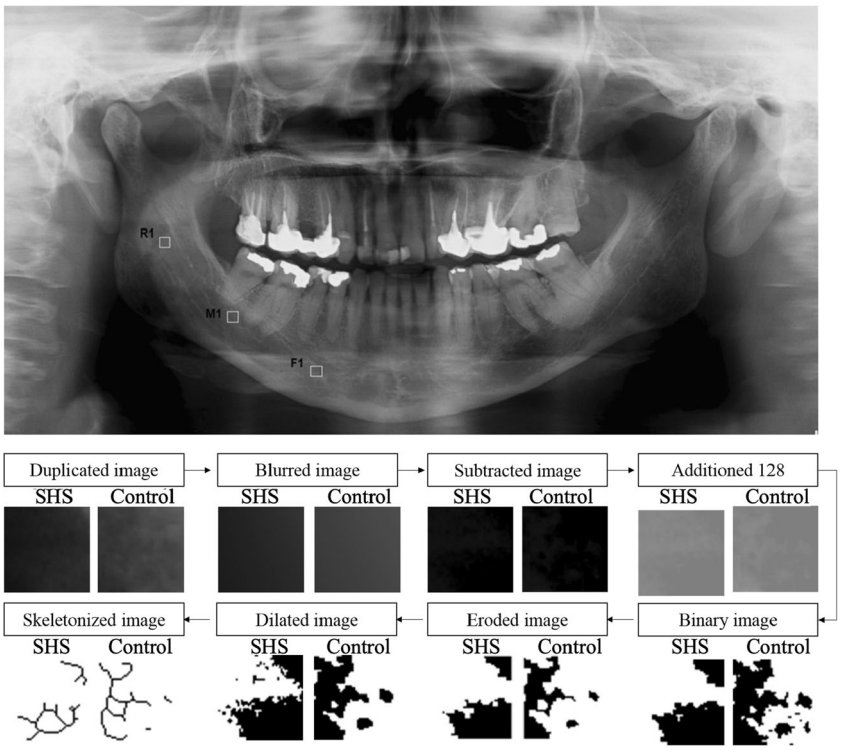

Fig. 1 Panoramic radiograph showing the regions of interest (ROIs) and an illustrative scheme of the methodology used to assess bone texture imaging parameters

performed simple randomization of the images by using a computer-generated list of random numbers ("randbetween" function of the Microsoft Excel). The statistician was also blinded since he did not know the images groups.

Evaluation of image texture parameters

Each image was segmented by using the MATLAB Release 2016a program to obtain the following standardized 50 × 50 pixels of ROIs on the mandibular right side (Fig. 1): F1—area delimited in the region of alveolar bone, located between the mental foramen and mandibular cortical bone; M1—region below and between first and second molars (the center area horizontally 2 cm from the intersection point of the oblique line and ramus in cases with missing right mandibular molars); and R1—geometric center of mandibular ramus [23]. These ROIs were analyzed using an algorithm based on the White and Rudolph [28] study.

Initially, a low-pass filter (Gaussian filter) was applied to reduce the image noise, using the kernel as $e^{\frac{-(x^2+y^2)}{2\sigma^2}} \Big/ 2\pi\sigma^2$ and $\sigma = 35$.Then, the blurred image was subtracted from the original image of each analyzed ROI. The resulting image received an additional gray value of 128 and it was made a binary. For this purpose, the Bradley algorithm was used, which considers each pixel of the image to be black if its brightness is k% lower than the average brightness of adjacent pixels [[29]]. By means of this process, the regions representing the bone trabeculae were evidenced with the black color and the intertrabecular spaces with the white color. Afterwards, the resulting image was eroded, dilated, and finally skeletonized with the purpose of determining the values of fractal dimension (d_f), lacunarity, and morphological characteristics adopted for the present study.

In order to calculate the fractal dimension, the algorithm of counting cells (box counting) was used according to the method described by White and Rudolph [28]. The choice of the box-counting method was due to its ease of use in mathematical calculations and experimental measurements. This method considers the ROI covered by a set of squares and, therefore, calculates the number of squares required to cover the entire ROI. The quantity of square is represented by $N(s)$, being "s" the scale, which represents the number of times that the side of the image would be divided. In this context, the calculation of the fractal dimension was done in the following way: $d_f = \frac{\log N(s)}{\log \frac{1}{s}}$.

Regarding lacunarity, the medullary region was similarly examined by inverting the image (making the marrow area as black color) and, then, skeletonizing the resulting image to its core marrow structure. In our customized algorithm, gray image pre-processing was performed using the automatic toolbox limit. This procedure allows a better reconstruction of the ROI aiming to establish an adequate threshold.

In addition, some morphological characteristics were obtained from each binary image [28]: (1) trabecular region = total number of black pixels divided by the total number of pixels in the region of interest; (2) periphery = number of pixels at the outer border of the trabeculae, which corresponds to a proportion of the total area of the trabeculae or the total ROI. From the skeletal image, the following were obtained: (1) total length of skeletal trabeculae (represented by the total number of black pixels), (2) number of end points (represented by the free ends, that is, each black pixel with only one adjacent black pixel), (3) number of branching points (represented by crossing points, i.e., each black pixel with 3 or more adjacent black pixels). These parameters were expressed as a ratio of trabecular length, area, and perimeter.

Bias

As an observational study, the following main factors that could bias the results were avoided [30]: selection and information bias, and measurement error. In order to avoid/minimize the occurrence of selection bias, patients were recruited regardless of the severity of osteometabolic alterations that they might present, and efforts were made to recruit all patients in routine care during the medical outpatient clinic. To avoid/minimize the occurrence of information bias, a detailed anamnesis and careful analysis of the medical records were performed in order to obtain consistent data. To avoid/minimize the occurrence of measurement bias, images were randomized and evaluated in a double-blind design, and the reliability of the measurements was assessed. In addition, TIFF format was adopted for each image since Yasar et al. [31] had found statistically significant difference between TIFF and JPEG images regarding the fractal dimension.

Study size

SHS is a rare disease and its incidence usually ranges from 0.2 to 2.8 cases per 100,000 women in developed countries [32]. Agarwal et al. [13] observed that patients with SHS had a lower bone mineral density in comparison with age- and sex-matched individuals of the control group (0.64 ± 0.09 versus 0.73 ± 0.11). Thus, based on this study, it was considered to evaluate a minimum of 27 patients per study group aiming to obtain a sample with 90% power at a 95% confidence interval. Regarding the possibility of sample loss during the study, 10% was added over the minimum sample calculation previously described, rendering 30 patients per group.

Reliability

To evaluate measurement reliability [33], the following analyses were performed: (1) intraclass correlation coefficient (ICC) statistics to assess systematic errors related to quantitative variables; (2) Dahlberg's formula to observe random errors of the measurements. Regarding the first one, the bidirectional ICC model of random effects was used with a confidence interval of 95% and a significant level of 5%. To evaluate possible technical errors, the Dahlberg formula was represented as $\sqrt{\frac{\sum d^2}{2n}}$, where $\sum d2$ is the sum of the squared differences between the two sets of two mean values, and "n" is the number of double measurements.

Statistical methods

Data were statistically analyzed by using the statistical program Statistical Package for the Social Sciences (IBM®, San Diego, CA, USA). Initially, data were submitted to the Kolmogorov-Smirnov normality test, and then the results were expressed as the mean and standard deviation (SD) of the mean. Comparisons between groups (control and SHS) and subgroups (SHS individuals aged up to 65 years or > 65 years) were performed using the Mann-Whitney test. Comparisons between fractal analyses were performed by the Wilcoxon test corrected by Bonferroni adjustment. General linear model (GLM) multivariate analysis was used in comparisons between control and SHS groups to reduce bias of multiple parameters.

To assess the predictive rate of different cutoff values of bone texture parameters in SHS group, a receiver operating characteristics (ROC) curve with obtained area under the curve (AUC) was constructed, and values of cutoff, sensitivity, and specificity were calculated. The subjects were classified based on the median of SHS diagnosis delay in years: ≤ 10 years, and > 10 years. Subsequently, we performed group-wise comparison through the Mann-Whitney test and obtained the AUC ROC curve.

A short-term precision study was conducted to assess the reproducibility of repeated measurements according to Glüer et al. [34], and standard deviation (SD), coefficient of variation (CV), and root mean square standard deviation (RMSSD) were obtained. A significance level of 5% was adopted.

Results

Regarding the reliability and reproducibility of the panoramic measurements, these errors of measurement were considered acceptable. It was observed an ICC average measure ranged from satisfactory ($r = 0.792$) to very satisfactory ($r = 0.910$), and the Dahlberg coefficient ranged from 0.008 to 0.463. Regarding the power of the sample based on the F1 fractal dimension value, comparing individuals in the control group (1.85 ± 0.01) and SHS patients (1.45 ± 0.73), an 85.1% power was estimated to reject the null hypothesis. Also, the short-term precision study analysis (Supplementary Table 1) showed no RSSD values higher than 2 in relation to the means 1 and 2. There was no group with a coefficient of variation higher than 25%. Only the repeated measure in ROI R1 presented CV near the maximum value (24.28%).

The sample comprised women with low educational level and poor socioeconomic status, and among them, 76.6% were postmenopausal at the time of dental evaluation. The patient's age range was 40 to 86 years (mean age of 64.5 ± 9.19 years), and age distribution by decade was as follows: 40–50 years ($n = 3$), 51–60 years ($n = 8$), 61–70 years ($n = 10$), 71–80 years ($n = 8$), > 81 years ($n = 1$). Regarding diseases with impact on bone metabolism, the hypothyroidism (100%), FSH/LH deficiency (73.33%), cortisol deficiency (86.66%), and growth hormone deficiency (93.33%) were described.

About the practice of physical activities, domestic activity was recorded in the majority of patients and regular practice of any physical exercise was absent in all patients. Clinically, high risk for osteoporosis was considered in all patients due to the presence of confirmed hypopituitarism. Regarding the obstetric findings, home delivery in 50% of the patients and obstetric complications

Table 1 Fractal dimension and lacunarity values

ROI	Group Parameters	Control	SHS	p value[a]	p value[b]
Region between the mental foramen and mandibular cortical bone (F1)	Fractal dimension	1.85 ± 0.01	1.47 ± 0.72	0.016*	0.004*
	Lacunarity	0.90 ± 0.33	0.85 ± 0.37	0.740	0.526
Region between first and second molars (M1)	Fractal dimension	1.68 ± 0.51	1.52 ± 0.67	0.043*	0.282
	Lacunarity	0.99 ± 0.17	0.96 ± 0.32	0.220	0.166
Geometric center of mandibular ramus (R1)	Fractal dimension	1.74 ± 0.42	1.68 ± 0.50	0.028*	0.277
	Lacunarity	0.90 ± 0.32	0.97 ± 0.23	0.008*	0.163

ROI, region of interest; *$p < 0.05$; [a] Mann-Whitney test; [b] GLM Multivariate analysis (mean ± SD)

Table 2 Morphological features related to the trabecular bone

	F1				M1				R1			
	Control	SHS	*p* value[a]	*p* value[b]	Control	SHS	*p* value[a]	*p* value[b]	Control	SHS	*p* value[a]	*p* value[b]
Trabecular area/total area	0.58 ± 0.04	0.57 ± 0.04	0.537	0.288	0.60 ± 0.05	0.57 ± 0.03	0.004*	0.008*	0.60 ± 0.06	0.58 ± 0.04	0.130	0.136
Periphery/total area	0.42 ± 0.04	0.43 ± 0.04	0.537	0.288	0.40 ± 0.05	0.43 ± 0.03	0.004*	0.008*	0.40 ± 0.06	0.42 ± 0.04	0.130	0.136
Periphery/trabecular area	0.72 ± 0.13	0.75 ± 0.11	0.679	0.438	0.66 ± 0.13	0.75 ± 0.09	0.004*	0.008*	0.68 ± 0.15	0.73 ± 0.11	0.138	0.187
Length/trabecular area	0.27 ± 0.05	0.29 ± 0.03	0.259	0.162	0.29 ± 0.06	0.32 ± 0.03	0.029*	0.025*	0.30 ± 0.06	0.32 ± 0.04	0.080	0.095
Length/total area	0.16 ± 0.02	0.16 ± 0.01	0.204	0.116	0.17 ± 0.02	0.18 ± 0.02	0.243	0.104	0.17 ± 0.02	0.18 ± 0.02	0.052	0.071
Terminal points/cm^2	0.12 ± 0.02	0.12 ± 0.01	0.557	0.388	0.13 ± 0.02	0.14 ± 0.02	0.286	0.172	0.13 ± 0.02	0.14 ± 0.02	0.036*	0.074
Terminal points/length	0.76 ± 0.03	0.76 ± 0.05	0.835	0.854	0.75 ± 0.04	0.76 ± 0.04	0.795	0.435	0.76 ± 0.04	0.78 ± 0.04	0.129	0.218
Terminal points/periphery	0.29 ± 0.04	0.29 ± 0.03	0.755	0.682	0.33 ± 0.04	0.32 ± 0.03	0.528	0.708	0.33 ± 0.03	0.34 ± 0.03	0.354	0.421
Terminal points/trabecular area	0.21 ± 0.05	0.22 ± 0.04	0.463	0.314	0.22 ± 0.05	0.24 ± 0.03	0.068	0.055	0.23 ± 0.05	0.25 ± 0.04	0.064	0.112
Branch points/cm^2	0.15 ± 0.02	0.16 ± 0.01	0.491	0.280	0.17 ± 0.02	0.17 ± 0.02	0.256	0.179	0.17 ± 0.02	0.18 ± 0.02	0.068	0.113
Branchs points/length	0.97 ± 0.01	0.96 ± 0.01	0.040*	0.073	0.97 ± 0.02	0.97 ± 0.01	0.256	0.404	0.97 ± 0.01	0.97 ± 0.01	0.611	0.739
Branch points/periphery	0.36 ± 0.04	0.37 ± 0.04	0.749	0.692	0.42 ± 0.05	0.41 ± 0.04	0.265	0.444	0.42 ± 0.03	0.42 ± 0.04	0.766	0.939
Branch points/trabecular area	0.26 ± 0.05	0.28 ± 0.04	0.354	0.220	0.28 ± 0.05	0.31 ± 0.03	0.032*	0.026*	0.29 ± 0.06	0.31 ± 0.04	0.106	0.098
Branch points/terminal points	1.16 ± 0.36	1.12 ± 0.40	0.705	0.700	1.14 ± 0.41	1.19 ± 0.31	0.756	0.580	1.23 ± 0.22	1.13 ± 0.36	0.184	0.216

ROI, region of interest; *$p < 0.05$; [a] Mann-Whitney test; [b] GLM Multivariate analysis (mean ± SD)

in 86.67% of the cases were reported. The age of the patients in reference to that at last delivery involving SHS-related obstetric events was 23–40 years (mean, 29.87 ± 5.52 years). Delay in the diagnosis of SHS represented by the time elapsed between the last birth and age of diagnosis was 1–31 years (mean, 10.79 ± 9.07 years).

Fractal dimension differed significantly between the studied groups. It was observed that its values measured at the region below the mental foramen ($p = 0.016$), region between lower molars ($p = 0.043$), and at the center of mandibular ramus ($p = 0.028$) were statistically lower in the SHS group when compared with the control group (Table 1). Regarding the lacunarity, it was observed that its mean value in mandibular ramus center region ($p = 0.008$) was statistically higher in SHS group (Table 1).

In relation to morphologic features that characterized the trabeculae, the mean value of branch points/length measurement ($p = 0.040$) in the mental foramen region was significantly lower in the SHS group (Table 2). In the molar region, the trabecular area/total area ($p = 0.004$), periphery/total area ($p = 0.004$), periphery/trabecular area ($p = 0.004$), and length/trabecular area ($p = 0.029$) were significantly higher in the study group (Table 4). In the central region of the mandibular ramus, terminal point/cm^2 was statistically higher ($p = 0.036$) in the SHS group when compared with the control group (Table 2).

When the morphological trabecular aspects were compared between the ROIs (Table 3), the region related to the mental foramen showed lower values of length/trabecular area, length/total area, terminal points/cm^2, terminal points/periphery, terminal points/trabecular area, branch points/cm^2, branch points/periphery, and branch points/trabecular area in comparison with the other ROIs ($p < 0.05$). The branch points/periphery showed a lower value in the region between the molars than in the central region of the mandibular ramus, which was statistically significant ($p < 0.05$).

The cumulative effect of all measurements of trabecular area parameters (Table 4) showed higher values of trabecular area/total area ($p = 0.026$), periphery/total area ($p = 0.026$), periphery/trabecular area ($p = 0.026$), length/trabecular area ($p = 0.018$), length/total area ($p = 0.049$), terminal points/cm^2 ($p = 0.026$), and branch points/trabecular area ($p = 0.008$) in SHS group. The age showed a direct association with lacunarity in mental foramen region ($p = 0.035$), as well as terminal points/periphery ($p = 0.005$) and branch points/cm^2 ($p = 0.025$) in molar region between SHS individuals. In addition, the branch points/terminal points ($p = 0.027$) in molar region showed an indirect association with age (Table 5).

In a multivariate analysis, only the mental foramen region ($p = 0.004$), trabecular area/total area ($p = 0.008$) (Table 1), periphery/total area ($p = 0.008$), periphery/trabecular area ($p = 0.008$), length/trabecular area ($p = 0.025$), and branch points/trabecular area ($p = 0.026$) (Table 2) remained with a statistically significant association. All cumulative measures that showed statistically significant association in bivariate analysis remained associated (Table 4).

The AUC value in ROC curve of the fractal analysis-derived parameters is shown in Supplementary material and Fig. 2. Moderate sensitivity and specificity were achieved for most of the parameters. Regarding fractal dimension, the mean value of all ROIs and mean of the F1 region had AUC of 0.700 and 0.701, respectively. Cutoff points over 0.18, and sensitivity and specificity of 64% were obtained. AUC for the R1 region in relation to the lacunarity of 0.720 was achieved; cutoff value < 0.10 and sensitivity and specificity of 68% were obtained.

Table 3 Comparison of the severity of fractal dimension, lacunarity, and morphological parameters between the ROIs in women with SHS

	F1 × M1	*p* value	F1 × R1	*p* value	M1 × R1	*p* value
Fractal dimension	–	0.107	–	0.136	–	0.975
Lacunarity	Reduced in F1	0.019*	reduced in R1	< 0.001*	Reduced in M1	0.018*
Trabecular area/total area	–	0.693	–	0.455	–	0.250
Periphery/total area	–	0.693	–	0.455	–	0.250
Periphery/trabecular area	–	0.940	–	0.673	–	0.172
Length/trabecular area	Reduced in F1	0.001*	Reduced in F1	0.001*	–	0.444
Length/total area	Reduced in F1	< 0.001*	Reduced in F1	< 0.001*	–	0.075
Terminal points/cm^2	Reduced in F1	0.003*	Reduced in F1	< 0.001*	–	0.146
Terminal points/length	–	0.656	–	0.117	–	0.144
Terminal points/periphery	reduced in F1	0.002*	reduced in F1	< 0.001*	reduced in M1	0.015*
Terminal points/trabecular area	reduced in F1	0.029*	reduced in F1	0.002*	–	0.221
Branch points/cm^2	reduced in F1	< 0.001*	reduced in F1	< 0.001*	–	0.467
Branchs points/length	–	0.158	–	0.973	–	0.206
Branch points/periphery	reduced in F1	< 0.001*	reduced in F1	< 0.001*	–	0.052
Branch points/trabecular area	reduced in F1	0.002*	reduced in F1	0.001*	–	0.549
Branch points/terminal points	–	0.683	–	0.315	–	0.374

*$p < 0.05$; Wilcoxon test (mean ± SD); –, meaning without difference

Table 4 Comparison of the cumulative effect (mean of the sum) of all morphological parameters from each of the analyzed ROIs between the control group and SHS group

	Group			
	Control	SHS	*p* value[a]	*p* value[b]
Trabecular area/total area	0.59 ± 0.04	0.57 ± 0.03	0.026*	0.025*
Periphery/total area	0.41 ± 0.04	0.43 ± 0.03	0.026*	0.025*
Periphery/trabecular area	0.69 ± 0.11	0.74 ± 0.08	0.035*	0.035*
Length/trabecular area	0.28 ± 0.05	0.31 ± 0.03	0.018*	0.017*
Length/total area	0.17 ± 0.02	0.18 ± 0.01	0.049*	0.049*
Terminal points/cm^2	0.13 ± 0.02	0.13 ± 0.01	0.089	0.088
Terminal points/length	0.76 ± 0.03	0.77 ± 0.03	0.256	0.256
Terminal points/periphery	0.31 ± 0.02	0.32 ± 0.02	0.747	0.800
Terminal points/trabecular area	0.22 ± 0.04	0.24 ± 0.03	0.060	0.066
Branch points/cm^2	0.16 ± 0.02	0.17 ± 0.01	0.067	0.070
Branchs points/length	0.97 ± 0.01	0.97 ± 0.01	1.000	1.000
Branch points/periphery	0.40 ± 0.02	0.40 ± 0.03	0.756	0.756
Branch points/trabecular area	0.27 ± 0.05	0.30 ± 0.03	0.026*	0.022*
Branch points/terminal points	1.18 ± 0.21	1.15 ± 0.21	0.613	0.600

*$p < 0.05$; [a] Mann-Whitney test; [b] GLM Multivariate analysis (mean ± SD)

The relationship between delay in SHS diagnosis and bone textural parameters (Supplementary Table 3) showed that the delay in SHS diagnosis showed a significant influence on the following morphologic features: trabecular area/total area ($p = 0.049$) in M1, periphery/total area ($p = 0.049$) in M1, terminal points/length in M1 ($p = 0.040$) and in the mean of the ROIs (0.017), and branch points/terminal points in F1 ($p = 0.012$) and in the mean of the ROIs ($p = 0.003$).

As illustrated in Fig. 3, the highest AUC was found to the mean branch points/terminal points (0.877 ± 0.076). Branch points/terminal points (0.823 ± 0.092) in F1, trabecular area/total area (0.750 ± 0.109) and periphery/total area (0.750 ± 0.109) in M1, and mean terminal points/length (0.805 ± 0.096) also presented acceptable predicting values of altered bone structure in SHS regarding delay in its diagnosis.

Table 5 Bone texture imaging parameters according to SHS age groups (up to 65 and > 65 years)

	F1			M1			R1		
	Up to 65 years	> 65 years	*p* value	Up to 65 years	> 65 years	*p* value	Up to 65 years	> 65 years	*p* value
Fractal dimension	1.71 ± 0.51	1.34 ± 0.80	0.173	1.33 ± 0.80	1.71 ± 0.46	0.154	1.71 ± 0.46	1.59 ± 0.62	0.558
Lacunarity	0.67 ± 0.47	0.95 ± 0.26	0.035*	0.88 ± 0.35	0.88 ± 0.36	0.970	1.03 ± 0.00	0.96 ± 0.26	0.334
Trabecular area/total area	0.56 ± 0.04	0.57 ± 0.05	0.649	0.57 ± 0.04	0.57 ± 0.02	1.000	0.58 ± 0.05	0.58 ± 0.03	0.616
Periphery/total area	0.44 ± 0.04	0.43 ± 0.05	0.649	0.43 ± 0.04	0.43 ± 0.02	1.000	0.42 ± 0.05	0.42 ± 0.03	0.616
Periphery/trabecular area	0.76 ± 0.10	0.74 ± 0.12	0.633	0.75 ± 0.11	0.75 ± 0.07	0.967	0.72 ± 0.15	0.74 ± 0.09	0.711
Length/trabecular area	0.29 ± 0.03	0.28 ± 0.04	0.508	0.30 ± 0.04	0.32 ± 0.02	0.142	0.32 ± 0.06	0.32 ± 0.03	0.934
Length/total area	0.17 ± 0.01	0.16 ± 0.01	0.334	0.17 ± 0.02	0.18 ± 0.01	0.084	0.19 ± 0.02	0.19 ± 0.01	0.914
Terminal points/cm^2	0.13 ± 0.01	0.12 ± 0.01	0.408	0.13 ± 0.02	0.14 ± 0.01	0.008*	0.14 ± 0.02	0.14 ± 0.02	0.849
Terminal points/length	0.77 ± 0.04	0.76 ± 0.06	0.632	0.74 ± 0.05	0.78 ± 0.02	0.019*	0.78 ± 0.05	0.77 ± 0.03	0.795
Terminal points/periphery	0.29 ± 0.03	0.29 ± 0.03	0.704	0.30 ± 0.04	0.34 ± 0.01	0.005*	0.35 ± 0.04	0.34 ± 0.03	0.497
Terminal points/trabecular area	0.23 ± 0.03	0.22 ± 0.04	0.414	0.23 ± 0.04	0.25 ± 0.02	0.069	0.25 ± 0.06	0.25 ± 0.03	0.968
Branch points/cm^2	0.16 ± 0.01	0.16 ± 0.01	0.623	0.17 ± 0.02	0.18 ± 0.01	0.025*	0.18 ± 0.02	0.18 ± 0.01	0.917
Branchs points/length	0.97 ± 0.01	0.96 ± 0.01	0.381	0.97 ± 0.01	0.97 ± 0.01	0.292	0.97 ± 0.02	0.97 ± 0.01	1.000
Branch points/periphery	0.37 ± 0.03	0.36 ± 0.04	0.866	0.40 ± 0.04	0.42 ± 0.02	0.102	0.43 ± 0.04	0.42 ± 0.03	0.328
Branch points/trabecular area	0.28 ± 0.04	0.27 ± 0.04	0.395	0.30 ± 0.04	0.31 ± 0.02	0.237	0.31 ± 0.06	0.31 ± 0.03	0.934
Branch points/terminal points	1.17 ± 0.32	1.10 ± 0.44	0.632	1.31 ± 0.08	1.24 ± 0.04	0.027*	1.16 ± 0.32	1.07 ± 0.44	0.538

*$p < 0.05$; Mann-Whitney test (mean ± SD)

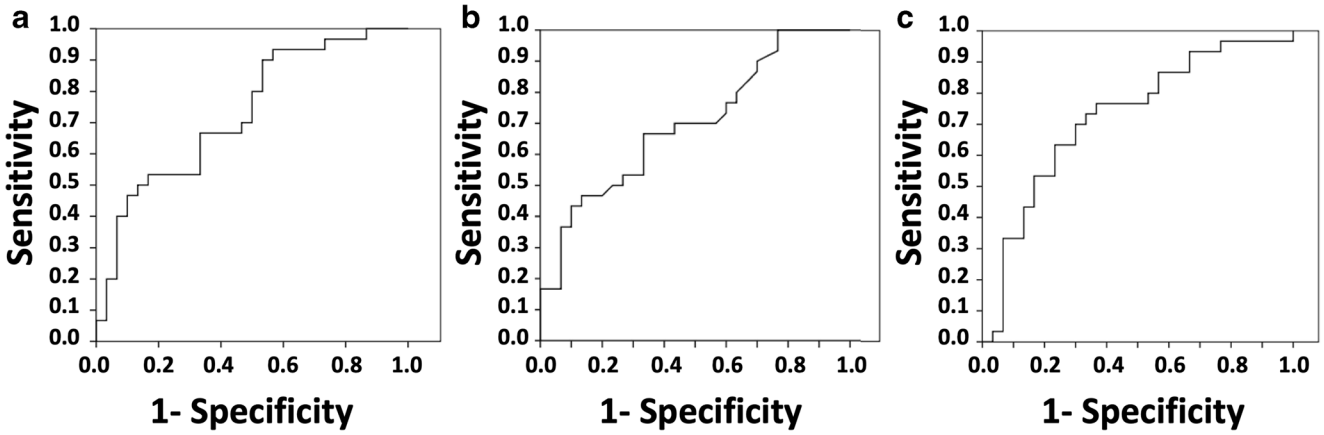

Fig. 2 The ROC curves of the fractal analysis-derived parameters. **a** Mean fractal dimension considering all ROIs. **b**) Fractal dimension in F1. **c** Lacunarity in R1

Discussion

Several investigations focusing on systemic disorders and its relationships with jawbones sites have performed texture analyses by using fractal dimension investigation in individuals affected by systemic disorders. To date, there are no published studies that evaluated the fractal dimension in SHS, which may reflect the altered bone metabolism in this disease due to pituitary failure [35].

The evaluation of bone density in patients with SHS is a relevant topic. However, scarce data has been addressed to the literature, since only 4 studies provided data of bone mass in

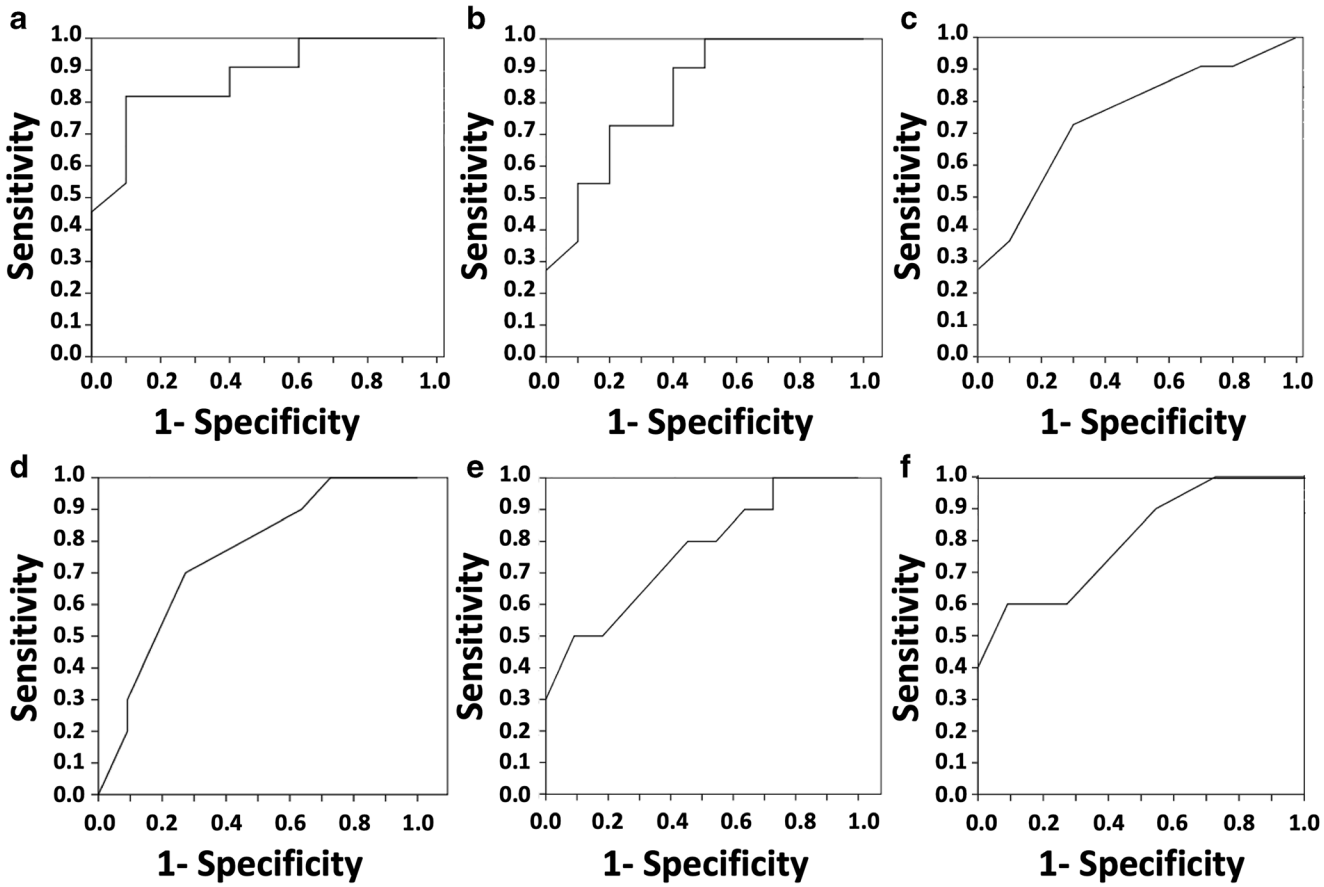

Fig. 3 The ROC curves of the relationship between delay in SHS diagnosis and bone textural parameters. **a** Mean branch points/terminal points considering all ROIs. **b** Branch points/terminal points in F1. **c** Trabecular area/total area in M1. **d** Periphery/total area. **e** Terminal points/length. **f** Mean terminal points/length considering all ROIs

women affected by this endocrine disease compared with control individuals [5, 13, 35, 36]. Agarwal et al. [13] reported 47% of SHS individual with low bone mass (Z-score ≤ -2.0) and 48% presenting with osteoporosis (T-score ≤ 2.5). Chihaoui et al. [35] described low bone mineral density in 46 endocrine patients (25 with osteopenia and 21 osteoporosis). Acibucu et al. [36] found 61.8% of the patients with osteoporosis and osteopenia in 32.3% of the remaining individuals. Gokalp et al. [5] studied premenopausal and postmenopausal SHS patients and observed lower T- and Z-scores for both femur and spine (L1–L5) compared with controls. The present case-control study could not obtain data about the bone mineral density of the patients, which has been considered a determinant aspect to provide bone strength [37]. However, in the present study, for the first time in SHS, a mandibular fractal analysis was performed, aiming to provide a suitable statistical bone texture analysis, which reflects the bone texture roughness and gray-level variations [37]. Pothuaud et al. [38] demonstrated that fractal analysis of bone texture can distinguish cases with an established diagnosis of osteoporosis from healthy controls.

Methods to calculate the fractal dimension include the yard stick, box counting, variation, structure-function, root mean square, fractional Brownian motion, and R/S analysis methods, and through each method, a different value of fractal dimension is obtained [39]. The box-counting algorithm is a mathematical method in which different square grids of 52–1664-μm size are overlapped on the ROI, and the number of boxes containing the edge of the binary image is expressed as the fractal dimension through linear regression method on log-log scale [18, 39]. This approach presents the advantage of having a widespread use in fractal analysis [18]. Also, it allows more homogenous comparison of the fractal dimension between studies that used this method [40]. Based on these findings, box counting was selected as the adequate method for our study.

The present study adopted fractal analysis as a method for estimating the texture of the mandibular trabeculae in specific ROIs, since it represents a useful mathematical method to analyze complex structures such as the trabecular bone [20, 25]. Selection of ROIs in the panoramic images was performed based on previous reports [23], and considered suitable regions to be submitted for fractal analysis. Panoramic X-ray is not considered a standardized imaging technique [23]. Nevertheless, the evaluated regions presented no significant distortion. The boxes were planned to attain standard dimensions for each ROI without overlapping of other anatomical structures.

Our study used mid-sized ROIs in agreement with previous studies [19, 20, 25] that showed significant values of fractal dimension based on validated methodologies. The ROI size of 50×50 pixels in the premolar region showed a statistically significant difference of the fractal dimension in osteoporotic women [22]. Moreover, as panoramic radiographs are not high-resolution images, the present study used TIFF format without compression to minimize this limitation and enable greater reliability of the fractal parameters [31].

This investigation used direct digital images for obtaining fractal dimension because some findings support that absence of film processing or imaging digitalization reduces the loss of image information, enhancing the texture parameter measurements reproducibility [37]. In addition, panoramic radiograph was used to assess bone trabecular microarchitecture in SHS because it has been shown to be a useful radiographic method for evaluating the reduction of bone mineral in the field of maxillofacial imaging, as well as it is a low-cost and easy to access exam routinely requested in dentistry [41].

It has been pointed out that the osteoporotic state reduces trabecular complexity and decreases the fractal dimension value [40]. The present results support this finding since a statistically significant difference between SHS and control groups was seen. SHS individuals presented low values of fractal dimension (mean of 1.54) compared with the control group, and this finding agreed with the results of similar investigations that used panoramic radiographs in osteoporotic state-related systemic diseases. Demirbas et al. [25] performed fractal analysis on panoramic radiographs of 35 individuals with sickle cell anemia and showed that the value of fractal dimension value in these individuals was significantly lower (mean of 1.68) in comparison with the control group. Sindeaux et al. [22] found that values of fractal dimension on mandibular cortical bone lower (mean of 1.14–1.35) in women with no osteoporosis. Gumussoy et al. [19] reported a reduced mean fractal dimension value (1.37) in a group of 25 patients with chronic renal failure in comparison with healthy individuals. In patients with temporomandibular disorder-related osteoarthritic changes, fractal dimension value decreased (mean of 1.22) as the severity of degenerative changes increased, showing that erosive and sclerotic condyles had an altered trabecular pattern [15].

Since higher bone turnover usually leads to trabecular bone loss, lower fractal dimension was expected in the more trabecular regions of the ROI in the mandibular ramus than the alveolar bone area of the selected ROI at the mental foramen. In individual ROIs analysis, contrary to expectation, the region with the highest content of trabecular bone (R1) presented the highest fractal dimension value, while the area with the lowest content of trabecular bone (F1) presented a lower fractal dimension value as previously observed [23]. However, this finding should be interpreted with caution, since the comparison of this parameter between the ROIs revealed no statistically significant difference between F1 and M1, F1 and R1, or M1 and R1. Thus, further investigation is needed to provide details of this finding in SHS.

Data presented in this report support the hypothesis that patients with SHS have an altered trabecular pattern in the

mandible, including morphologic aspects obtained from the binary and skeletonized images of the selected regions of interest. For instance, each morphological parameter evaluated in this investigation described a specific organizational pattern of the pixels and was relevant to demonstrate differences between individuals with and without osteoporosis [28, 41, 42]. Collectively, the parameters reflect the degree of bone complexity of the selected area as reported in the previous study [26]. The finding of more significant decrease of these features is considered to indicate lower complexity in the studied region, which may be interpreted as bone loss in the clinical setting [41, 42].

It was found moderate sensitivity and specificity of the bone texture variables for predicting low structure in the mandible of SHS subjects. Alman et al. [17] reported that panoramic radiographs showed moderate sensitivity and specificity for fractal dimension in discriminating patients based on DXA values. Presently, for characterizing osteoporotic and non-osteoporotic individuals, assessment of bone mineral density was not possible. However, fractal dimension was associated with moderate sensitivity and specificity in differentiating SHS and controls. To improve the sensitivity and specificity of combined textural bone parameters [42] on panoramic radiographs of SHS patients, further studies assessing the bone mineral density by DXA are required.

A decrease in the architectural complexity of SHS patients was observed that resembled a similar osteoporotic state as observed in panoramic radiographs of osteoporotic individuals evaluated by White and Rudolph [28]. SHS individuals showed statistically significant lower values of the trabecular area, periphery, and skeletal length in comparison with the control group, as previously observed in osteoporotic subjects [28]. In this study, the number of terminal points did not differ in comparison with non-SHS patients on the base of the statistical analysis. We believe that this finding may reflect a lower severity of mandibular trabecular alteration presented in this sample of SHS individuals as compared with the results obtained from White and Rudolph [28] study, which highlighted that the number of terminal points is a suitable indicator of bone resorption state in the jawbones of osteoporotic patients. Also, the measures of branch points were statistically decreased in SHS, which reflects the core trabecular structure as previously observed [28]. Although some trabeculae morphologic features did not show the statistically significant difference in the SHS group, even decreased in comparison with the control group, this finding was observed in a group of postmenopausal women with low bone mineral density assessed by DXA [42].

In the present study, the diagnosis delay found among the individuals with SHS was 10.79 ± 9.07 years. This finding was similar to data presented by Ramiandrasoa et al. [43] since they described a mean delay of 9 ± 9.7 years in a sample of 39 women diagnosed with SHS. Acibucu et al. [36] reported a delay between the final delivery and the diagnosis of 21.29 ± 7.7 years, and they considered that this longer period of hormonal alteration provoked a negative impact on the bone in SHS subjects. Stockholm et al. [44] support the hypothesis that this diagnosis delay occurs because SHS is a chronic disease. In this context, we also believe that the lower fractal dimension values and altered morphologic features observed in this investigation probably were a consequence of the negative effect of a delayed diagnosis on the bone mass content loss over the years and the socioeconomic position that could influence in a nutritional deficit. Bone mineral density has been compromised in SHS because these patients usually are diagnosed with hypopituitarism at a young age, and they develop important nutritional deficiency [45], which is significantly affected by the socio-economic status-related risk factors, including calcium, protein, and vitamin D intake [46]. This finding was previously discussed by our group in an observational study with SHS individuals, who showed a remarkable lower socio-economic strata [47].

This study has some limitations. Digital panoramic radiography is a 2D image of a 3D structure [19]. This imaging exam is usually affected by anatomical superpositions (e.g., hyoid bone and ghost images) and image distortions due to the acquisition technique [15]. ROI selection was set at areas under less influence of image distortion, mainly due to overlapping structures according to a previous report [23]. Furthermore, panoramic radiographs are routine and low-cost exams requested by dentists, which can detect cases of suspicious osteoporosis based on fractal analysis parameters and clinical data, and such patients are subsequently referred for proper medical evaluation.

Regarding fractal analysis, the obtained results should be interpreted with some caution because it was not possible to compare the data with reference values of bone mineral density assessment, such as DXA. However, a significant difference between patients with SHS and controls was obtained, which reflects an altered bone pattern commonly observed in other osteoporotic disorders. Another study limitation was that fractal analysis has restriction regarding the absence of threshold values such as T-scores obtained through DXA. To the best of our knowledge, this is the first study to report cutoff values for panoramic radiograph-related bone texture parameters in patients with SHS.

Reports have indicated that binary process to obtain textural parameters was associated with some loss of detailed information [18]; however, in all ROIs, the loss was homogenous because both the imaging process and analysis program were standardized. Fractal dimension calculated with customized computer program algorithm may be influenced by selection of adequate threshold value. To comply with this workflow imaging process-associated operational requirement, binary imaging with threshold brightness value of 128 was performed as previously reported [28]. Regarding the studied

population, there was some concern with respect to sample size and female predominance; however, SHS is a rare disease that affects only women [32].

Furthermore, according to the International Society For Clinical Densitometry guidance [48], BMD studies should consider during DXA interpretation the %CV-derived least significant change (LSC), which represent the precision error (%CV) × 2.77. For clinical practice, LSC should not exceed pre-determined values for the lumbar spine, total hip, and femoral neck. Although this study had found high %CVs in panoramic radiographs of SHS individuals, which would overestimate reasonable values for LSC, it should be interpreted with some caution. To date, there are no validated case-control studies that have recommended clinically acceptable LSC values for panoramic radiographs.

In conclusion, based on the findings of the present novel research, the SHS sample studied was characterized by a decrease in fractal dimension and some morphologic features, which may be a reflection of a possible reduced bone mineral density in these individuals due to osteometabolic changes that occurred over the years since the onset of the systemic manifestations associated with the postpartum hemorrhage. We believe fractal analysis may be an alternative and useful tool for improving the diagnostic capacity of panoramic radiography on mandibular changes of individuals with SHS. Also, it is necessary that further SHS studies in the field of the maxillofacial imaginology be done, especially those correlating bone texture aspects and bone mineral density by DXA.

Funding This study was supported by the Institutional Program for Scientific Initiation Scholarships – National Council for Scientific and Technological Development (PIBIC-CNPq), Brazil.

Compliance with ethical standards

Ethical approval This study was approved by the Ethics Committee of the Federal University of Ceará (research protocol # 983 022).

Conflicts of interest None.

References

1. Imam A, Iqbal J, Blair HC, Davies TF, Huang CL, Zallone A, Zaidi M, Sun L (2009) Role of the pituitary-bone axis in skeletal pathophysiology. Curr Opin Endocrinol Diabetes Obes 16:423–429
2. Colaianni G, Cuscito C, Colucci S (2013) FSH and TSH in the regulation of bone mass: the pituitary/immune/bone axis. Clin Dev Immunol 2013:382698
3. Zaidi M, Sun L, Liu P, Davies TF, New M, Zallone A, Yuen T (2016) Pituitary-bone connection in skeletal regulation. Horm Mol Biol Clin Investig 28:85–94
4. Sheehan HL (1937) Postpartum necrosis of the anterior pituitary. J Pathol Bacteriol 45:189–214
5. Gokalp D, Tuzcu A, Bahceci M, Arikan S, Ozmen CA, Cil T (2009) Sheehan's syndrome and its impact on bone mineral density. Gynecol Endocrinol 25:344–349
6. Karaca Z, Laway BA, Dokmetas HS, Atmaca H, Kelestimur F (2016) Sheehan syndrome. Nat Rev Dis Primers 22:16092
7. Haddock L, Vega LA, Aguiló F, Rodríguez O (1972) Adrenocortical, thyroidal and human growth hormone reserve in Sheehan's syndrome. Johns Hopkins Med J 131:80–99
8. Keleştimur F (2003) Sheehan's syndrome. Pituitary 6:181–188
9. Bolanowski M, Halupczok J, Jawiarczyk-Przybyłowska A (2015) Pituitary disorders and osteoporosis. Int J Endocrinol 2015:206853
10. Sert M, Tetiker T, Kirim S, Kocak M (2003) Clinical report of 28 patients with Sheehan's syndrome. Endocr J 50:297–301
11. Dökmetaş HS, Kilicli F, Korkmaz S, Yonem O (2006) Characteristic features of 20 patients with Sheehan's syndrome. Gynecol Endocrinol 22:279–283
12. Diri H, Tanriverdi F, Karaca Z, Senol S, Unluhizarci K, Durak AC, Atmaca H, Kelestimur F (2014) Extensive investigation of 114 patients with Sheehan's syndrome: a continuing disorder. Eur J Endocrinol 171:311–318
13. Agarwal P, Gomez R, Bhatia E, Yadav S (2019) Decreased bone mineral density in women with Sheehan's syndrome and improvement following oestrogen replacement and nutritional supplementation. J Bone Miner Metab 37:171–178
14. Shevroja E, Lamy O, Kohlmeier L, Koromani F, Rivadeneira F, Hans D (2017) Use of trabecular bone score (TBS) as a complementary approach to dual-energy X-ray absorptiometry (DXA) for fracture risk assessment in clinical practice. J Clin Densitom 20:334–345
15. Arsan B, Köse TE, Çene E, Özcan İ (2017) Assessment of the trabecular structure of mandibular condyles in patients with temporomandibular disorders using fractal analysis. Oral Surg Oral Med Oral Pathol Oral Radiol 123:382–391
16. Servais JA, Gaalaas L, Lunos S, Beiraghi S, Larson BE, Leon-Salazar V (2018) Alternative cone-beam computed tomography method for the analysis of bone density around impacted maxillary canines. Am J Orthod Dentofac Orthop 154:442–449
17. Alman AC, Johnson LR, Calverley DC, Grunwald GK, Lezotte DC, Hokanson JE (2012) Diagnostic capabilities of fractal dimension and mandibular cortical width to identify men and women with decreased bone mineral density. Osteoporos Int 23:1631–1636
18. Yasar F, Akgünlü F (2005) Fractal dimension and lacunarity analysis of dental radiographs. Dentomaxillofac Radiol 34:261–267
19. Gumussoy I, Miloglu O, Cankaya E, Bayrakdar IS (2016) Fractal properties of the trabecular pattern of the mandible in chronic renal failure. Dentomaxillofac Radiol 45:20150389
20. Apolinário AC, Sindeaux R, de Souza Figueiredo PT, Guimarães AT, Acevedo AC, Castro LC, de Paula AP, de Paula LM, de Melo NS, Leite AF (2016) Dental panoramic indices and fractal dimension measurements in osteogenesis imperfecta children under pamidronate treatment. Dentomaxillofac Radiol 45:20150400
21. Shrout MK, Potter BJ, Hildebolt CF (1997) The effect of image variations on fractal dimension calculations. Oral Surg Oral Med Oral Pathol Oral Radiol Endod 84:96–100
22. Sindeaux R, Figueiredo PT, de Melo NS, Guimarães AT, Lazarte L, Pereira FB, de Paula AP, Leite AF (2014) Fractal dimension and mandibular cortical width in normal and osteoporotic men and women. Maturitas 77:142–148
23. Hwang JJ, Lee JH, Han SS, Kim YH, Jeong HG, Choi YJ, Park W (2017) Strut analysis for osteoporosis detection model using dental panoramic radiography. Dentomaxillofac Radiol 46:20170006
24. Ergün S, Saraçoglu A, Güneri P, Ozpinar B (2009) Application of fractal analysis in hyperparathyroidism. Dentomaxillofac Radiol 38:281–288
25. Demirbaş AK, Ergün S, Güneri P, Aktener BO, Boyacioğlu H (2008) Mandibular bone changes in sickle cell anemia: fractal

analysis. Oral Surg Oral Med Oral Pathol Oral Radiol Endod 106: e41–e48
26. Kurşun-Çakmak EŞ, Bayrak S (2018) Comparison of fractal dimension analysis and panoramic-based radiomorphometric indices in the assessment of mandibular bone changes in patients with type 1 and type 2 diabetes mellitus. Oral Surg Oral Med Oral Pathol Oral Radiol 126:184–191
27. Rondon RH, Pereira YC, do Nascimento GC (2014) Common positioning errors in panoramic radiography: a review. Imaging Sci Dent 44:1–6
28. White SC, Rudolph DJ (1999) Alterations of the trabecular pattern of the jaws in patients with osteoporosis. Oral Surg Oral Med Oral Pathol Oral Radiol Endod 88:628–635
29. Bradley D, Roth G (2007) Adaptative thresholding using the integral image. Journal of Graphics Tools 12:13–21
30. Hammer GP, du Prel JB, Blettner M (2009) Avoiding bias in observational studies: part 8 in a series of articles on evaluation of scientific publications. Dtsch Arztebl Int 106:664–668
31. Yasar F, Apaydin B, Yilmaz HH (2012) The effects of image compression on quantitative measurements of digital panoramic radiographs. Med Oral Patol Oral Cir Bucal 17:1074–1081
32. Kovacs K (2003) Sheehan syndrome. Lancet 361:520–522
33. Harris EF, Smith RN (2009) Accounting for measurement error: a critical but often overlooked process. Arch Oral Biol 54:S107–S117
34. Glüer CC, Blake G, Lu Y, Blunt BA, Jergas M, Genant HK (1195) Accurate assessment of precision errors: how to measure the reproducibility of bone densitometry techniques. Osteoporos Int 5:262–270
35. Chihaoui M, Yazidi M, Chaker F, Belouidhnine M, Kanoun F, Lamine F, Ftouhi B, Sahli H, Slimane H (2016) Bone mineral density in Sheehan's syndrome; prevalence of low bone mass and associated factors. J Clin Densitom 19:413–418
36. Acibucu F, Kilicli F, Dokmetas HS (2014) Assessment of bone mineral density in patients with Sheehan's syndrome. Gynecol Endocrinol 30:532–535
37. Lespessailles E, Gadois C, Lemineur G, Do-Huu JP, Benhamou L (2007) Bone texture analysis on direct digital radiographic images: precision study and relationship with bone mineral density at the os calcis. Calcif Tissue Int 80:97–102
38. Pothuaud L, Lespessailles E, Harba R, Jennane R, Royant V, Eynard E, Benhamou CL (1998) Fractal analysis of trabecular bone texture on radiographs: discriminant value in postmenopausal osteoporosis. Osteoporos Int 8:618–625
39. Liang Z, Feng Z, Guangxiang X (2012) Comparison of fractal dimension calculation methods for channel bed profiles. Procedia Eng 28:252–257
40. Updike SX, Nowzari H (2008) Fractal analysis of dental radiographs to detect periodontitis-induced trabecular changes. J Periodontal Res 43:658–664
41. Lee BD, White SC (2005) Age and trabecular features of alveolar bone associated with osteoporosis. Oral Surg Oral Med Oral Pathol Oral Radiol Endod 100:92–98
42. Licks R, Licks V, Ourique F, Radke Bittencourt H, Fontanella V (2010) Development of a prediction tool for low bone mass based on clinical data and periapical radiography. Dentomaxillofac Radiol 39:224–230
43. Ramiandrasoa C, Castinetti F, Raingeard I, Fenichel P, Chabre O, Brue T, Courbière B (2013) Delayed diagnosis of Sheehan's syndrome in a developed country: a retrospective cohort study. Eur J Endocrinol 169:431–438
44. Stochholm K, Gravholt CH, Laursen T, Laurberg P, Andersen M, Kristensen LØ, Feldt-Rasmussen U, Christiansen JS, Frydenberg M, Green A (2007) Mortality and GH deficiency: a nationwide study. Eur J Endocrinol 157:9–18
45. Zargar AH, Singh B, Laway BA, Masoodi SR, Wani AI, Bashir MI (2005) Epidemiologic aspects of postpartum pituitary hypofunction (Sheehan's syndrome). Fertil Steril 84:523–528
46. Shatrugna V, Kulkarni B, Kumar PA, Rani KU, Balakrishna N (2005) Bone status of Indian women from a low-income group and its relationship to the nutritional status. Osteoporos Int 16: 1827–1835
47. Cavalcante DD, Pinto-Quidute AR, Alves-Martins MR, Walter-de-Aguiar AS, Lima-Cid AM, Silva PG, Cavalcante RF, Costa FW (2018) Dental status, salivary flow, and sociodemographic aspects in Sheehan Syndrome patients. Med Oral Patol Oral Cir Bucal 23: e436–e442
48. Lewiecki EM, Binkley N, Morgan SL, Shuhart CR, Camargos BM, Carey JJ, Gordon CM, Jankowski LG, Lee JK, Leslie WD; International Society for Clinical Densitometry (2016) Best practices for dual-energy X-ray absorptiometry measurement and reporting: International Society for Clinical Densitometry Guidance. J Clin Densitom 2016 19:127–140